Resistance switching and formation of a conductive bridge in metal/binary oxide/metal structure for memory devices

KOHEI FUJIWARA[1], TAKUMI NEMOTO[1], MARCELO J. ROZENBERG[1,2], YOSHINOBU NAKAMURA[1] AND HIDENORI TAKAGI[1,3,4*]

[1] Department of Advanced Materials and Department of Applied Chemistry, University of Tokyo, Kashiwa 277-8561, Japan

[2] Laboratoire de Physque des Solides, Université Paris-Sud, Orsay 91405 cedex, France

[3] Correlated Electron Research Center, National Institute of Advanced Industrial Science and Technology, Tsukuba 305-8562, Japan

[4] RIKEN (The Institute of Physical and Chemical Research), Wako 351-0198, Japan

Correspondence should be addressed to H. T. ([*]e-mail: htakagi@k.u-tokyo.ac.jp) or K .F. (kk57110@mail.ecc.u-tokyo.ac.jp).

The voltage-induced nonvolatile resistance switching recently reported in perovskite oxides[1,2] has triggered numerous studies in a variety of transition metal oxide materials to realize a new generation of nonvolatile memory devices with high speed and low power consumption, called Resistive Random Access Memory (ReRAM). While the resistance switching was initially believed to be specific to perovskite Mn oxides, it is now clear that this effect is a rather ubiquitous phenomenon of transition metal oxides. Among a wide variety of oxides, binary compounds, such as CuO, NiO, TiO_2 are particularly appealing materials for resistive memory devices due to their low cost, simple processing and compatibility with CMOS technology[3,4]. The resistance switching effect in oxide dielectrics produced by electric-field stress has been known since the 60's[5-10]. Many mechanisms have been proposed since then, however, the origin of the change in conductance remains elusive and is a main obstacle in regard of future application. The formation of conducting filaments within the insulating oxide has been suggested as an essential ingredient of resistance switching. Here we report the direct observation of a conducting bridge within the CuO channel of metal/CuO/metal planar-type resistance switching device, which is formed upon the initial voltage application. We find that the resistance switching phenomenon only occurs when just one single bridge is formed during a soft dielectric breakdown. We argue that the oxidation and reduction of this conducting bridge by the action of an applied field and/or current gives rise to a novel non-volatile memory effect. The location and size of the bridge were found to be controllable by appropriate design of the electrodes' geometry.

The structure of the resistance switching device, often called ReRAM, is very simple, consisting of a capacitor-like sandwich structure of metal/insulating oxide/metal. In devices with binary transition metal oxides, such as CuO, NiO[3,4], TiO_2[3,11], Fe_2O_3[12], and CoO_x[12,13], the resistance between the two metal electrodes shows a very sharp and reproducible switching from a high-resistance state (HRS) to a low-resistance state (LRS) at a threshold voltage V_{set} and switching from a LRS to a HRS at V_{reset}. These two processes are respectively called set and reset. Rather surprisingly, the switching is usually non-polar, that is, the transition occurs depending on the absolute value of the applied voltage and not on its polarity. Thus, a

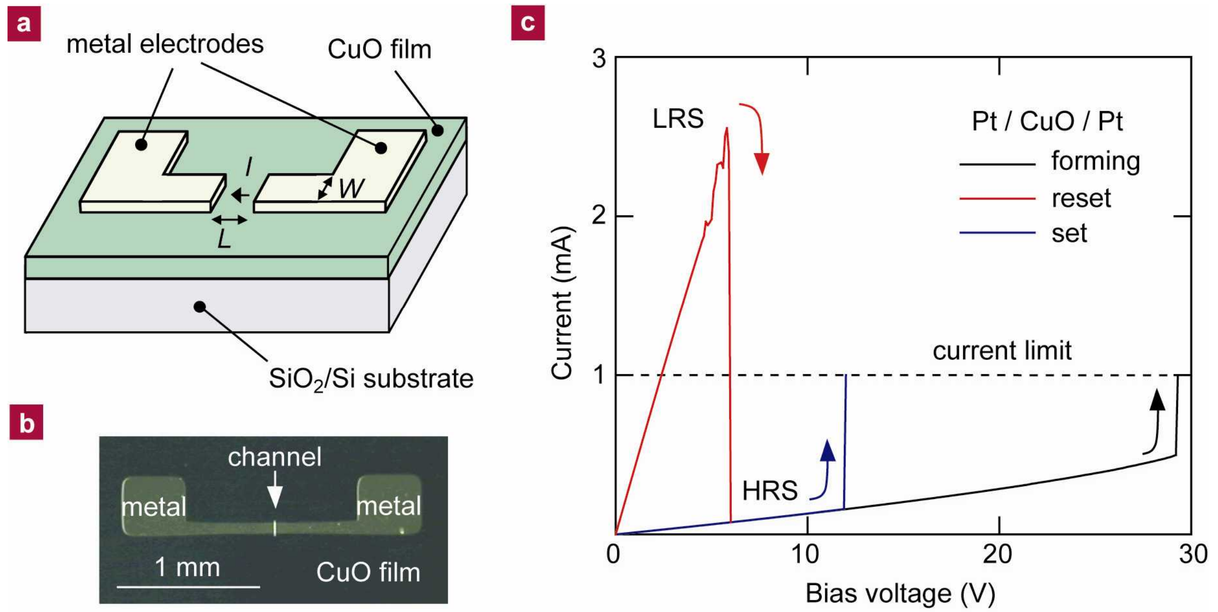

Figure 1. **Resistance switching in metal/CuO/metal structure. a,** The structure of device is schematically shown. Two metal (Pt) electrodes are placed on CuO film, forming Pt/CuO/Pt structure. Ni electrodes are also used. The channel length and width are represented as *L* and *W*, respectively. Current, *I,* is passed between the two metal electrodes. **b,** An optical microscopic image of a device from top view. The gap region between the two electrodes represents the CuO channel. **c,** The current *I* - voltage *V* curves for a Pt/CuO/Pt planar-type resistance switching device with a channel length of 2.1 μm and a channel width of 90 μm is shown. As prepared sample is in high resistance state (HRS) with resistance $R \sim 81$ kΩ (black curve). With increasing voltage, "forming" occurs at $V_{forming} = 29.3$ V, and the device switched to low resistance state (LRS) with $R \sim 2.4$ kΩ (red curve). With increasing voltage in the LRS, the device returns back to HRS at $V_{reset} = 6.0$ V (blue curve). The HRS can be switched back to the LRS again at $V_{set} = 12.0$ V ($< V_{forming}$). This switching between HRS and LRS occurs repeatably and independent of the polarity of applied voltage. These behaviors are in parallel to those of capacitor-type device reported previously[3,4,11-13,25-29].

device that has been switched with an applied voltage of a given polarity can be switched back by the successive application of a voltage of the same or opposite polarity. Importantly, in order to initiate this memory operation, an initial voltage $V_{forming}$, larger than V_{set} and V_{reset} , must be applied to the as prepared device. This device activation process is called forming.

Proposed mechanisms for the resistance switching effect that emerged from recent research include polarity-dependent oxygen diffusion[14-16], Schottky barrier controlled by charge accumulation at the interface[17], resistance switching at dislocation[18], pulse-generated crystalline defect[19,20], carrier trapping[21], internal doping effect by a change of a dopant valence state[22] and Mott transition at the electrode interface based on theoretical model calculations[23-25]. Closely linked with these models, in the particular case of the resistance switching in binary oxides, the existence of a filamentary conductive path responsible for the effect has been speculated since the early work on NiO films[6]. Many recent studies have provided indirect evidences for the formation of conductive filaments within the dielectric[11,26-31]. For example, it was reported that the resistance of the LRS does not depend on the area of the metal electrode, while that of the HRS scales with the inverse of electrode area[12,27]. This implies that the current flow should be

spatially inhomogeneous in the LRS but not in the HRS. This can be qualitatively understood assuming the existence of a current path, with a much smaller section than the length scale of electrodes, which allows or blocks the current for each of the two resistance states. In this study, we attempt to directly image the putative inhomogeneous spatial structure of conducting path and, more importantly, to disclose the nature of the path formation and the current blocking mechanism.

To directly access the observation of the oxide dielectric connected to metal electrodes, we have fabricated metal/CuO/metal (metal = Pt and Ni) planar-type devices rather than the usual stacked-capacitor-type devices (see Methods). In these devices, two metal electrodes are fabricated on top of CuO film as shown schematically in Fig. 1(a). An optical microscope image of a metal/CuO/metal device is shown in Fig. 1(b). The current-voltage characteristics of the planar-type device were essentially the same as those observed in the conventional capacitor-type devices studied previously[3,4,11-13,26-30]. Figure 1(c) shows typical data for a sample with Pt metal electrodes. Upon the first application of voltage, forming is observed at V_{forming} ~ 29.3 V and the system switches to the LRS. To protect the device, a current limit was set at 1 mA. Under the application of successive voltage ramps of the same polarity, the reset from the LRS to the HRS is observed at V_{reset} ~ 6.0 V, and the set from the HRS to the LRS is observed at V_{set} ~ 12.0 V. These voltages are smaller than the forming voltage, verifying $V_{\mathrm{forming}} > V_{\mathrm{set}} > V_{\mathrm{reset}}$. Note that the strength of these threshold voltages is roughly about one order of magnitude larger than those observed in conventional capacitor devices. This difference, however, can be naturally understood as due to the sample geometry. In particular, the separation between the two metal electrodes is of the order of a hundred nanometers for capacitor structures, while it is about a few micrometers in the present case. In addition, all the specific peculiarities of the switching phenomenon reported in conventional capacitor-type devices are also observed in our system. For instance, current fluctuations when V_{reset} is approached in the reset transition[28], and that the observed values of resistance in the HRS were always very close to those of the as prepared sample, while the values in the LRS were typically about two orders smaller. These features give strong support to the implicit assumption that the physical mechanism responsible for the resistance switching phenomenon in the present planar sample is essentially the same as the one in the previously studied capacitor-like structures.

To investigate the conjectured formation of a conducting path, we first focus on the forming process where a most dramatic change in the structure can be anticipated. The observed forming voltages in samples having various channel lengths (electrode distance) and width are summarized in figure 2(a). The linear increase of forming voltage with channel length, and its independence respect to the channel width, imply that the forming process is essentially driven by the electric-field strength between the two electrodes. The slope of a linear fit of the data yields a forming electric-field of 1.46×10^{5} V/cm. The same linear dependence of forming voltage with the thickness of the dielectric oxide layer (equivalent to the channel length here) was observed in the capacitor-type devices[3] with a corresponding magnitude of electric-field comparable to those observed in the present planar-type devices. We should also mention here that these electric-field strengths agree reasonably well with usual values for dielectric breakdown of transition metal oxide insulators[32,33].

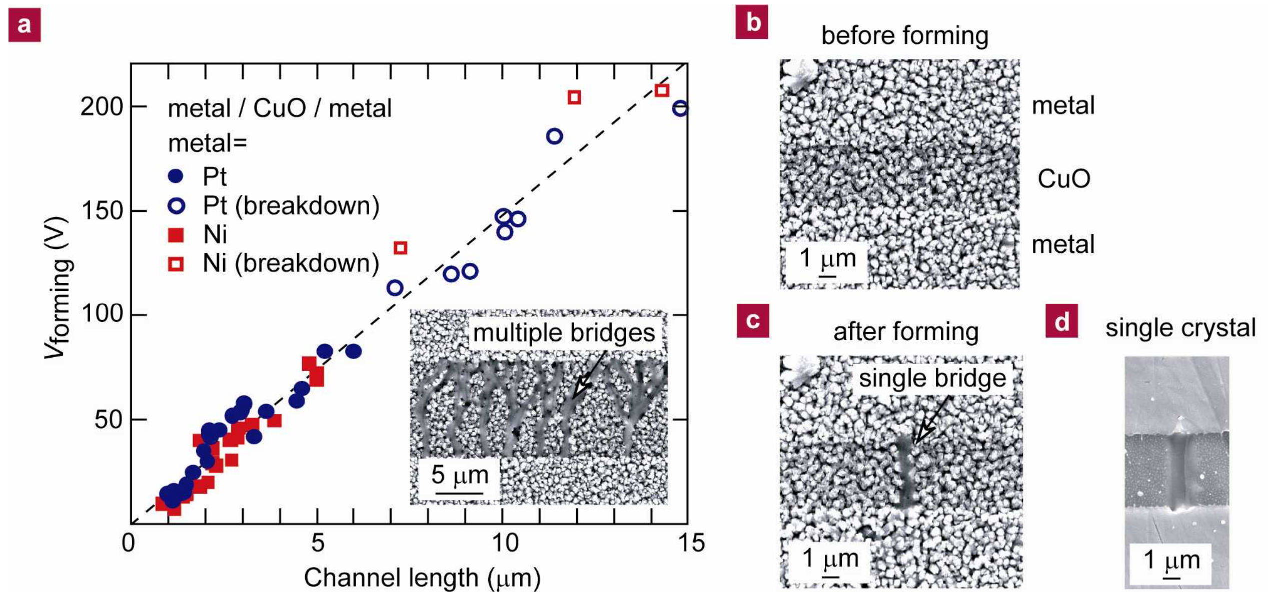

Figure 2. **Bridge formation within CuO channel by forming process. a,** The forming operation (the first application of voltage on as prepared sample) was performed on metal/CuO/metal (metal = Pt and Ni) resistance switching devices formed on sputtered CuO films. The channel length (electrode distance) dependence of forming voltage is shown for devices with various channel widths (70 ~ 120 μm) using filled symbols. The universal linear behavior indicates the electric-field (~ 1.46×10^5 V/cm) is driving the forming. **b,** The SEM image of a Ni/CuO/Ni device with a channel length of 4.0 μm and a width of 110 μm before the forming are partially shown. The bright region represents the two Ni-coated electrode areas and the dark gap region does the CuO channel. **c,** After the forming, a bridge-like structure with a width of 1 μm is formed between the two Ni electrodes, see also Figure 3, where an enlarged picture of bridge is shown. When the channel length is larger than 7 μm, a permanent breakdown of device was observed. The SEM image in the inset of panel (a) represents the case for permanent breakdown, where we observe the formation of multiple bridges. The voltages for such permanent breakdown were also plotted in panel (a) as opened symbols. We clearly see that the forming voltages fall onto a universal line together with the breakdown voltages, indicating the physical origin of the two seemingly different operations are the same. **d,** The SEM image of a Pt/CuO/Pt device after forming fabricated on the surface of CuO bulk single crystal instead of polycrystalline film in (b) and (c). The channel length and width were 4.5 μm and 110 μm, respectively. The formation of bridge structure is clearly observed, implying that the bridge formation does not depend on the micro structure of CuO channel.

Figure 2(b) shows the scanning electron microscopy (SEM) image of a section of the CuO insulator surface between the Ni electrodes. We observe a noticeable change in the SEM image of the channel region after the forming: as shown in Fig.2(c), a single filament-like bridge structure with a width of about 1 μm showed up between the two metal electrodes. The bridge has the appearance of a melted region and was never present in the as prepared devices, thus it is due to the action of the forming process. Interestingly, whenever a sample showed reversible set and reset transitions, namely resistance switching operation, we almost invariably observed the presence of a single bridge in the channel. Cases where two bridges were present did occur, but remained rather exceptional. The bridge persisted without displaying any observable change in its SEM image after the device was reset to the HRS. We also

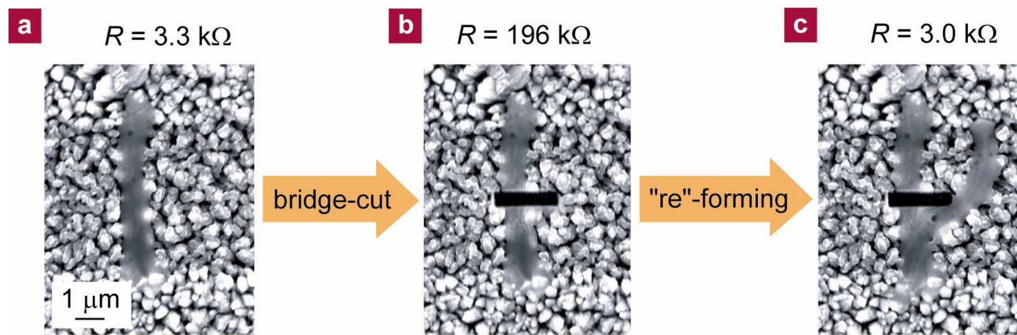

Figure 3. **Bridge-cut experiment. a,** The SEM image of conductive bridge and the resistance *R* between the two metal electrodes in a Ni/CuO/Ni resistance switching device before the bridge-cut. In between the dotted line is the CuO channel region. The channel length of this device was 5.2 μm and the width was 80 μm. After the forming, the bridge can be clearly seen and the resistance *R* was as low as 3 kΩ indicating the device is in the LRS. **b,** The bridge was then cut by creating a narrow slit like hole using focused ion beam. The resistance after the cut recovers its as prepared value ~ 200 kΩ. **c,** Then a "re"-forming was conducted after the cut and the *R* recovered the LRS value ~ 3 kΩ. In the corresponding SEM, branching of bridge is clearly recognized. These results indicate that the bridge observed is responsible for the conduction in the LRS.

fabricated similar planar-type devices on the surface of bulk CuO single crystals, and observed the same bridge structure and the resistance switching after forming as shown in Fig.2(d). This implies that the bridge formation does not depend on the micro structure of the insulating oxide.

In order to find direct evidence that the observed bridge is responsible for the conduction in the LRS, an experiment where the bridge was physically cut was conducted. The resistance (*R*) between the electrodes of the as prepared device shown in Fig. 3 was *R*~ 200 kΩ. After the forming, the device was found in the LRS with *R* = 3.3 kΩ and, in the SEM image, we could identify the single bridge shown in Fig. 3(a). We then physically cut the bridge by focused ion beam (FIB) process as shown in Fig. 3(b) and, without any voltage application, found that *R* recovered to 196 kΩ, the HRS. Note that the length of the cut slit was only a few μm, which is one order of magnitude smaller than the width of electrodes (i.e., of the channel) ~ 80 μm. Therefore, if the current in the LRS had been flowing in a region that extended significantly beyond the location of the bridge, we should not have observed the almost perfect recovery of *R* to the initial high resistance value of the insulating channel. The recovery of *R* to a value close to the HRS by bridge-cutting was reproduced in more than 10 devices. In addition, as a control experiment, instead of cutting the bridge, we cut the clean channel region a few μm away from the bridge, but in that case we did not observe any noticeable increase of *R*. These results clearly demonstrate that the current in the LRS does flow through the bridge structure formed by a soft breakdown. To further investigate the nature of the bridge, we attempted the re-forming of a device whose bridge had been previously cut, i.e., a 2nd forming process. We observed that the device regained its switching operation. In the SEM image after this 2nd forming we observed that the cut bridge developed a branch, reconnecting the electrodes, as shown in Fig. 3(c). This further demonstrates the metallic nature of the bridge structure and its key role in the switching phenomenon.

The bridge-cutting experiment was also performed on a device in the HRS. Only a small increase of R of a few percents was found, which can be ascribed to the reduction of effective channel width. This observation implies that in the HRS, the conduction through the bridge is essentially fully blocked. Since, as previously mentioned, the SEM images show that the bridge structure remains apparently unmodified after the reset transition, the bridge becomes electrically "dead" in the HRS. What effects are taking place within the bridge structure are then the key to understand the nature of the set and the reset process.

To investigate the physical nature of the different conduction states, the channel resistance in the LRS and HRS were measured as a function of temperature. Figure 4 shows a typical metallic behavior of the resistance observed in the LRS, where the current mostly flows through the bridge. In contrast, the resistance in both, the as prepared state and the HRS shows insulating behavior as displayed in the inset of Fig. 4. No appreciable difference was observed in $R(T)$ between the as prepared state and the HRS, again indicating that conduction within the bridge is completely blocked in HRS. It should be pointed out that pure Cu is the only metallic phase possible from a Cu-O binary system. This implies the presence of a Cu metal path inside the bridge. In support for this, the temperature dependence of $R(T)$, with a knee-like structure around 200 K associated to the Debye temperature, agrees very well with those reported for Cu metal[34,35]. The absence of electrode metal within the bridge was confirmed by energy dispersive X-ray analysis (EDX). An estimate of the resistivity in the LRS, assuming that the whole bridge structure contributes to the conduction homogeneously[36], gives ~ 2×10^{-2} Ω cm, which is too high to be consistent with the presence of bulk Cu. It is natural then to conclude

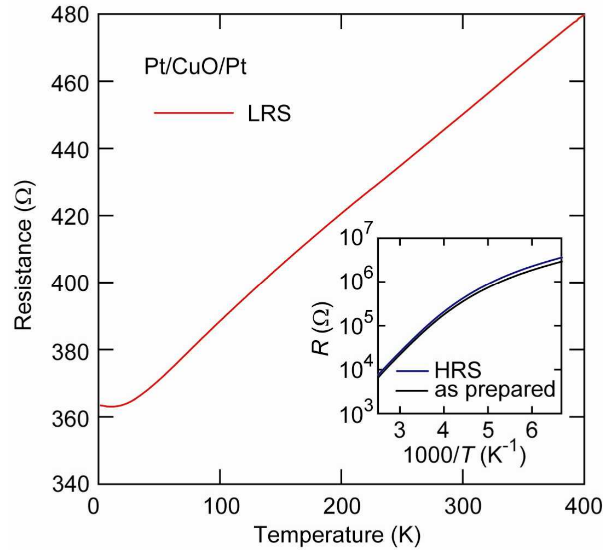

Figure 4. **Metal-insulator transition accompanied with resistance switching.** The temperature dependence of channel resistance $R(T)$ of a Pt/CuO/Pt resistance switching device with a channel length of 1.8 μm and a width of 95 μm was measured at each stage of resistance switching. The main panel shows $R(T)$ in the LRS indicating that the conduction is dominated by a good metal, highly likely Cu. The inset shows $R(T)$ in the as prepared state and in the HRS. From the temperature dependence an activation energy of ~ 0.14 eV was estimated.

that the bridge consists of a mixture of Cu and insulating CuO_x, and that minor Cu metal regions within the bridge give rise to a network of filamentary conduction paths in the LRS. The SEM-EDX analysis was not able to identify the presence of regions of Cu metal within the given spatial resolution, however the indication of reduced oxygen content within the bridge structure by ~ 10 % compared to the surrounding CuO channel is consistent with the presence of a fine CuO_x-Cu mixture. From the values of resistance observed in the LRS and those of pure Cu, one estimates that the cross section of the putative Cu filamentary path may be of order of a few tens of nanometers. This Cu filamentary path inside the bridge gets interrupted upon switching to the HRS,

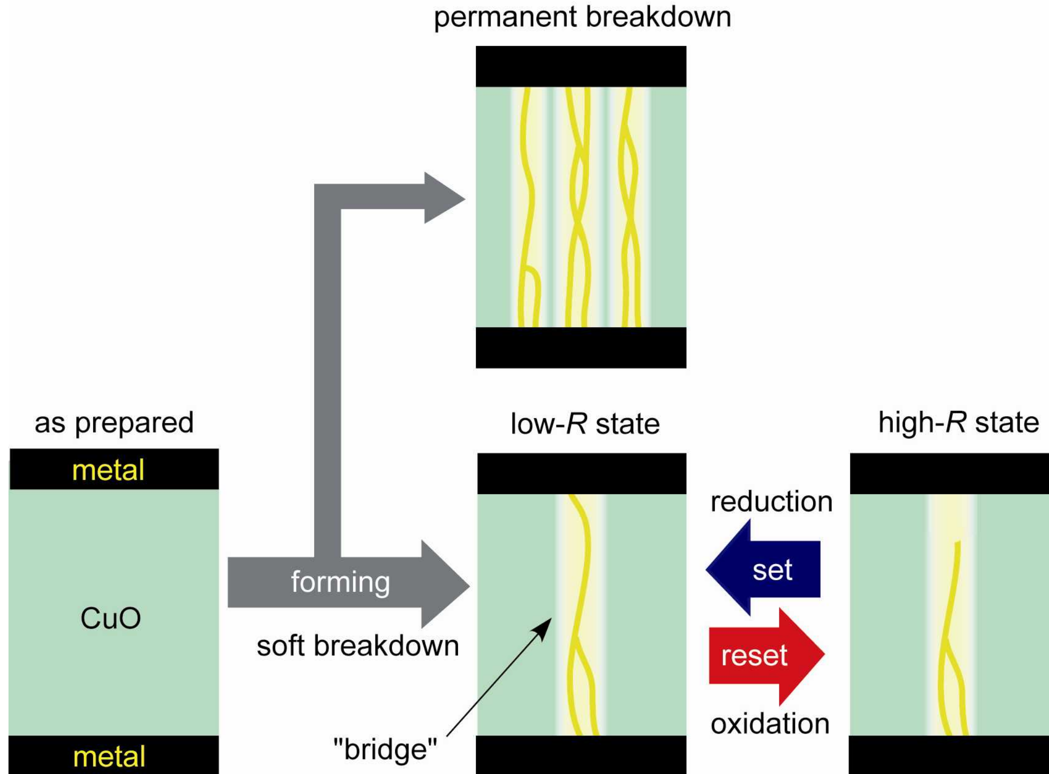

Figure 5. **Oxidation-reduction model for resistance switching.** The schematic image of resistance switching in real space proposed from the present study of metal/CuO/metal devices. The forming process creates a conducting bridge which is a mixture of filamentary Cu metal (yellow) and insulating oxide (white) by a soft breakdown. The filamentary Cu metal path can be blocked and opened repeatably by applying electric-field and/or current. If multiple bridges are produced in the forming, a permanent breakdown results. The set and reset voltages are found to be rather independent of the channel length as already reported for capacitor-type devices[12]. This might mean that the set and reset occur only in a segment of the filamentary path, possibly near the electrode interface region[12,24-26,29].

which may be reasonably ascribed to the re-oxidation of a segment of the Cu path.

Based on these experimental results, we propose a mechanism of resistance switching schematically described in Fig. 5. The forming is essentially a soft dielectric breakdown, which is an extremely fast process, where CuO is reduced within a single bridge-like structure. The conducting bridge, made of an insulating CuO_x melt with an embedded Cu metal network, is consequently formed. The conduction in the LRS is through the Cu metal network, and is suppressed during the reset process by the re-oxidation of a segment of the Cu metal network. The subsequent set transition is similar to the initial forming breakdown, but only occurs at the location of the re-oxidized segments (hence the smaller threshold voltage, $V_{set} < V_{forming}$) and the conduction of the Cu network is thus recovered by the chemical reduction of those segments. The scenario that we propose here can be viewed as a phase change memory action based on a local reduction-oxidation of CuO_x.

The microscopic mechanism of such reduction-oxidation process is not fully clear yet. Nevertheless, the reduction of CuO by plasma-induction for the remaking of Cu is a known method in metallurgy, thus one might imagine that a similar process occurs here

at the reduce scale of the device during its electric breakdown forming. On the other hand, the oxidation mechanism responsible for the reset might be more elusive. We suspect that it might be a form of current-driven oxidation. Indeed the maximal current density sustained during the reset is remarkably large, a lower bound of 10^6 A/cm^2 is estimated by assuming a homogeneous current flow over the whole bridge structure. It was reported that a high current density (10^7 A/cm^2) can induce a local oxidation of a Ti nano-wire that is constricted by a TiO_x anodized region[37,38]. The Ti nano-scale constriction surrounded by insulating TiO_x is in fact reminiscent of the proposed scenario of a conductive nano-scale network of Cu metal embedded within the insulating CuO_x melt of the bridge. One may therefore speculate that a similar oxidation process can occur in the CuO_x system.

An important issue for eventual application as memory device, is to control the position and the size of the formed bridge. In this respect, the observation made of the bridge branching and reconnecting to the electrode in a 2nd forming after the bridge-cut by FIB, suggests that the location of the bridge can be controlled by fabricating a metallic seed in the electrode for the soft dielectric breakdown. To further establish this point, we fabricated different types of seeds, such as a rectangular shaped protuberance and a pair of opposite triangular shaped electrodes, as shown in Fig. 6. After the forming, we clearly observed that the bridges were in fact formed at the seeds' locations, as indicated by the arrows in the figure. These images, demonstrate the feasibility of position control of the bridge. We note that when the gap between the electrodes was longer that 1 μm, the thickness of the bridge was of the order of 1 μm as shown in Figures 6(a) and (b). This bridge thickness is similar to the ones described previously for devices without seed (Figures 2 and 3). However, when two

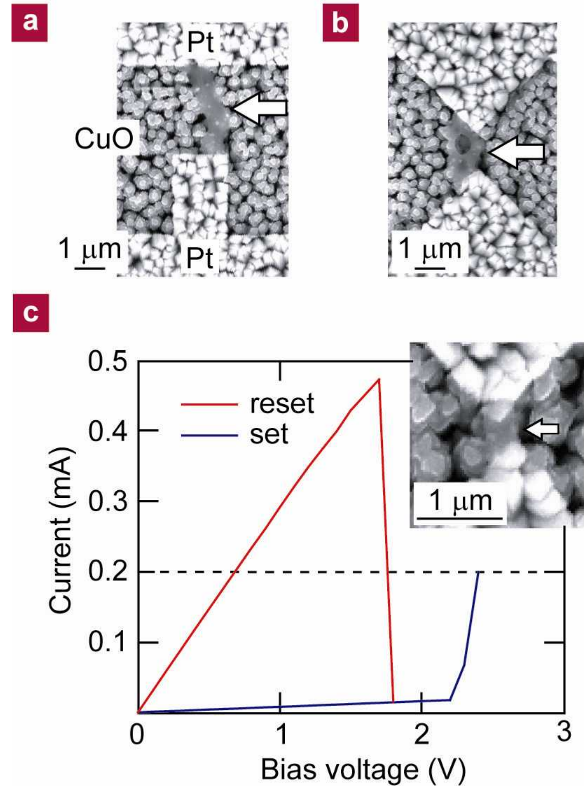

Figure 6. **Control of bridge size and position. a and b,** The SEM images of a Pt/CuO/Pt device with patterned electrodes for forming with a bridge seed. The images were taken after the forming process. The bridges were formed right at the seed electrodes, demonstrating that the location of the bridge formation can be controlled. **c,** Downsized seed electrodes produced a sub-micrometer bridge with enhanced *I-V* characteristics.

sharp triangular seeds were placed with a separation smaller than 1 μm, as shown in Fig. 6(c), the thickness of the bridge was significantly reduced and it appears to be of similar size as the grains of the polycrystalline film. Such reduction of the geometrical dimensions of the bridge resulted in the drastic improvement of the switching characteristics. The current-voltage characteristics of this device, shown in Fig 6(c), shows that the V_{set} and V_{reset} are now as small as 1-2 V, that is, one order of magnitude smaller than those of the devices with bridge length of over μm. This is a clear consequence of the combination of the sharp

triangular shapes of the seeds and their small separation. More remarkable is, perhaps, the reduction of the switching current by almost one order of magnitude compared with the other devices. This is likely due to the reduction of the cross-section of the bridge. The combination of these two features has the important consequence of a dramatic reduction the power consumption. Thus, from these results one might expect that the effect of downsizing this type of resistance switching memory would actually be to improve its operation specifications. This notable "the smaller, the better" performance of this binary oxide resistance switching device, we believe, is a very appealing feature in regard to possible future application. While the planar-type memory developed for this study was originally motivated for the exploration of the mechanism of resistance switching, these last results on the scalability of the device might open the way for the actual practical adoption of this geometry.

In summary, we fabricated planar-type metal/CuO/metal resistance switching devices. From the correlation between the observed electrical behavior and the real space image, we found that a single bridge-like path is generated within the CuO after "forming" through a soft dielectric breakdown process. The bridge was demonstrated to be responsible for the conduction in the low resistance state. The metallic temperature dependence of resistance in the low resistance state strongly suggests the presence of a Cu metal filament network embedded within the CuO_x bridge. We propose that the set and the reset switching are respectively associated to a reduction and oxidation of a narrow segment of the Cu metal path promoted by electric-field or current. The resistance switching device might be therefore considered as an electrochemical phase change memory. We demonstrated that the position and the dimensions of the bridge can be controlled by appropriate patterning of the electrodes' geometry. Finally, the observed improvements in the power dissipation requirements obtained by downscaling of the device demonstrates the high potential of binary oxide resistance switching for next generation nonvolatile memory applications.

Methods

Sample preparation

The metal/CuO/metal device structure used in this study was prepared using the following recipe. A CuO polycrystalline film of 2.6 μm thickness was grown on a SiO_2/Si substrate by radio-frequency magnetron sputtering with a 99.9 % pure CuO ceramic target. During the deposition, the temperature of substrate was kept at 300 ^{o}C and the pressure was fixed at 0.7 Pa of Ar-O_2 (96:4) gas. A Pt or Ni film with a thickness of 70 nm was deposited onto the CuO film by electron beam deposition, and then the channel was formed by creating a slit in the metal electrode using a focused ion beam processing system (JEOL JEM-9310FIB). The optical microscopic image of the obtained planar-type sample is shown in Fig. 1(b). The channel length (electrode distance) and channel width (electrode width) were ranged from 0.8 to 15 μm and from 70 to 110 μm, respectively.

Electrical measurements and surface observation

Current-voltage characteristics were measured at room temperature in air using a semiconductor parameter analyzer (Agilent Technologies 4155C) and a voltage-source meter (Keithley 237). The surface observation of CuO channel region in each stage of the resistance switching operation was conducted by scanning electron microscopy (SEM) (KEYENCE VE-7800). Energy dispersive X-ray (EDX) analysis was also performed for the mapping of the local composition

change of the channel region with an analyzer (EDAX Genesis 2000) equipped with the SEM system.

References

1. Liu, S. Q., Wu, N. J. & Ignatiev, A. Electric-pulse-induced reversible resistance change effect in magnetoresistive films. *Appl. Phys. Lett.* **76,** 2749-2751 (2000).

2. Beck, A., Bednorz, J. G., Gerber, Ch., Rossel, C. & Widmer, D. Reproducible switching effect in thin oxide films for memory application. *Appl. Phys. Lett.* **77,** 139-141 (2000).

3. Baek, I.G. *et al.* Highly scalable non-volatile resistive memory using simple binary oxide driven by asymmetric unipolar voltages pulses. *Tech. Dig. – Int. Electron Devices Meet.* **2004**, 587-590 (2004).

4. Seo, S. *et al.* Reproducible resistance switching in polycrystalline NiO films. *Appl. Phys. Lett.* **86,** 5655-5657 (2004).

5. Hickmott, T. W. Low-frequency negative resistance in thin anodic oxide films. *J. Appl. Phys.* **33,** 2669-2682 (1962).

6. Gibbons, J. F. & Beadle, W. E. Switching properties of thin NiO films. *Solid-State Electron.* **7**, 785-797 (1964).

7. Chopra, K. L. Avalanche-induced negative resistance in thin oxide films. *J. Appl. Phys.* **36**, 184-187 (1965).

8. Dearnaley, G., Stoneham, A. M. & Morgan, D. V. Electrical phenomena in amorphous oxide films. *Rep. Prog. Phys.* **33,** 1129-1191 (1970).

9. Oxley, D. P. Electroforming, switching and memory effects in oxide thin films. *Electrocomponent Sci. Tech.* **3**, 217-224 (1977).

10. Pagnia, H. & Sotnik, N. Bistable switching in electro-formed metal-insulator-metal devices. *Phys. Status Solidi* **108,** 11-65 (1988)

11. Choi., B. J. *et al.* Resistive switching mechanism of TiO_2 thin films grown by atomic-layer deposition. *J. Appl. Phys.* **98,** 033715 (2005)

12. Inoue, I. H., Yasuda, S., Akinaga, H. & Takagi, H. Nonpolar resistance switching of metal / binary-transition-metal oxides / metal sandwiches: homogeneous / inhomogeneous transition of current distribution. *cond-mat*/0702564 (2007). submitted to *Phys. Rev. B.*

13. Shima, H., Takano, F., Tamai, Y., Akinaga, H & Inoue., I. H. Synthesis and characterization of Pt/Co-O/Pt trilayer exhibiting large reproducible resistance switching. *Jpn. J. Appl. Phys.* **46,** L57-60 (2007).

14. Chen, X., Wu, N., Strozier, J. & Ignatiev, A. Spatially extended nature of resistive switching in perovskite oxide thin films. *Appl. Phys. Lett.* **89,** 063507 (2006)

15. Fujimoto, M. *et al.* TiO_2 anatase nanolayer on TiN thin film exhibiting high-speed bipolar resistive switching. *Appl. Phys. Lett.* **89,** 223509 (2006).

16. Quintero, M., Levy, P., Leyva, A. G. & Rozenberg M. J. Mechanism of Electric-Pulse-Induced Resistance Switching in Manganites. *Phys. Rev. Lett.* **98**, 116601 (2007).

17. Sawa, A., Fujii, T., Kawasaki, M. & Tokura, Y. Hysteretic current-voltage characteristics and resistance switching at a rectifying $Ti/Pr_{0.7}Ca_{0.3}MnO_3$ interface. *Appl. Phys. Lett.* **85,** 4073-4075 (2004).

18. Szot, K., Speier, W., Bihlmayer, G. & Waser, R. Switching the electrical resistance of individual dislocations in single-crystalline $SrTiO_3$. *Nature. Mater.* **5,** 312-320 (2006).

19. Tsui, S. *et al.* Field-induced resistive switching in metal-oxide interfaces. *Appl. Phys. Lett.* **85,** 317-319 (2004)

20. Hamaguchi, M., Aoyama, K., Asanuma, S., Uesu, Y. & Katsufuji, T. Electric-field-induced resistance switching universally observed in transition-metal-oxide thin films. *Appl. Phys. Lett.* **88,** 142508 (2006)

21. Odagawa, A. *et al.* Colossal electroresistance of a $Pr_{0.7}Ca_{0.3}MnO_3$ thin film at room temperature. *Phys. Rev. B* **70,** 224403 (2004).

22. Meijer, G. I. *et al.* Valence states of Cr and the insulator-to-metal transition in Cr-doped $SrTiO_3$. *Phys. Rev. B* **72,** 155102 (2005)

23. Oka, T. & Nagaosa, N., Interfaces of correlated electron systems: Proposed mechanism for colossal electroresistance. *Phys. Rev. Lett.* **95,** 266403 (2005).

24. Rozenberg, M. J., Inoue, I. H. & Sánchez, M. J. Nonvolatile memory with multilevel switching: A basic model. *Phys. Rev. Lett.* **92,** 178302 (2004).

25. Rozenberg, M. J., Inoue, I. H. & Sánchez, M. J. Strong electron correlation effects in non-volatile electronic memory devices. *Appl. Phys. Lett.* **88,** 033510 (2006).

26. Rohde, C. *et al.* Identification of a determining parameter for resistive switching of TiO_2 thin films. *Appl. Phys. Lett.* **86,** 262907 (2005).

27. Seo, S. *et al.* Conductivity switching characteristics and reset currents in NiO films. *Appl. Phys. Lett.* **86,** 093509 (2005).

28. Kim, D. C. *et al.* Electrical observations of filamentary conductions for the resistive memory switching in NiO films. *Appl. Phys. Lett.* **88,** 202102 (2006).

29. Kinoshita, K., Tamura, T., Aoki, M., Sugiyama Y. & Tanaka, H. Bias polarity dependent data retention of resistive random access memory consisting of binary transition metal oxide. *Appl. Phys. Lett.* **89,** 103509 (2006).

30. Kinoshita, K., Tamura, T., Aoki, M., Sugiyama Y. & Tanaka, H. Lowering the switching current of resistance random access memory using a herero junction structure consisting of transition metal oxides. *Jpn. J. Appl. Phys.* **45,** L991-994 (2006).

31. Rossel, C., Meijer, G. I., Brémaud, D. & Widmer, D. Electrical current distribution across a metal-insulator-metal structure during bistable switching. *J. Appl. Phys.* **90,** 2892-2898 (2001).

32. Klein, N. Switching and breakdown in films. *Thin Solid Films.* **7,** 149-177 (1970)

33. Fuschillo, N., Lalevic, B. & Leung, B. Electrical conduction and dielectric breakdown in crystalline NiO and NiO (Li) films. *J. Appl. Phys.* **46,** 310-316 (1975).

34. White, G. K. & Woods, S. B. Electrical and thermal resistivity of the transition elements at low temperatures. *Phil. Trans. Roy. Soc.* **251,** 273-302 (1959).

35. Moore, J. P., McElroy, D. L. & Graves, R. S. Thermal conductivity and electrical resistivity of high-purity copper from 78 to 400 ^{o}K. *Can. J. Phys.* **45,** 3849-3865 (1967).

36. In this estimation, we assume the depth of the bridge structure, which cannot be seen in our sample geometry, ~ 1 μm, almost equal to the width of the bridge observed. In the case of a depth of 100 nm, the estimated resistivity goes down to 2×10^{-3} Ωcm, which is still much higher than the value of bulk Cu metal.

37. Schmidt, T., Martel, R., Sandstrom, R. L. & Avouris, Ph. Current-induced local oxidation of metal films: Mechanism and quantum-size effects. *Appl. Phys. Lett.* **73,** 2173-2175 (1998).

38. Martel, R., Schmidt, T., Sandstrom, R. L. & Avouris, Ph. Current-induced nanochemistry: Local oxidation of thin metal films. *J. Vac. Sci. Technol.* A **17,** 1451-1456 (1999).

Acknowledgements

The authors would like to thank I. H. Inoue, H. Akinaga, A. Sawa, H. Y. Hwang, H. Akoh, M. Kawasaki and Y. Tokura for helpful discussions. This work is supported by a Grant-in-Aid for Scientific Research from MEXT, Japan (No. 19104008). One of the authors, K. F., acknowledges the support from Japan Society for the Promotion of Science.